We are IntechOpen, the world's leading publisher of Open Access books Built by scientists, for scientists

4,800
Open access books available

122,000
International authors and editors

135M
Downloads

Our authors are among the

154
Countries delivered to

TOP 1%
most cited scientists

12.2%
Contributors from top 500 universities

CLARIVATE ANALYTICS BOOK CITATION INDEX INDEXED

WEB OF SCIENCE™

Selection of our books indexed in the Book Citation Index in Web of Science™ Core Collection (BKCI)

Interested in publishing with us?
Contact book.department@intechopen.com

Numbers displayed above are based on latest data collected.
For more information visit www.intechopen.com

17

Multiscale Manufacturing of Three-Dimensional Polymer-Based Nanocomposite Structures

Louis Laberge Lebel and Daniel Therriault
École Polytechnique of Montreal, Canada

1. Introduction

There is currently a worldwide effort for advances in micro and nanotechnologies due to their high potential for technological applications in fields such as microelectromechanical systems (MEMS), organic electronics and high-performance structures for aerospace. In these fields, nanoparticle-filled composites, i.e. nanocomposites, represent an interesting material option compared to conventional resins due to their enhanced properties and multi-functional potential. However, several significant scientific and technological challenges must be first overcome in order to fabricate nanocomposite-based structures and devices rapidly and cost-effectively. Various fabrication techniques of one or two-dimensional (1D/2D) nanocomposite structures have been developed, but few techniques are available for three-dimensional (3D) nanocomposite structures. The capability to manufacture complex 3D structures will greatly expand the practical applications of nanocomposite materials and enable the development of novel devices such as a 3D nanocomposite micro-coil spring. This chapter will present an overview of the challenges in multiscale fabrication and the current manufacturing techniques available to create 3D structures of polymer-based nanocomposites.

2. A multiscale approach

Due to the several orders of magnitude involved in the fabrication of nanocomposite devices, an efficient manufacturing technique must address the challenges at the nano-, micro- and macroscales. Figure 1 shows this multiscale concept for the creation of a 3D scaffold structure using a single-walled carbon nanotube (SWNT) and a polymer nanocomposite.

At the nanoscale, the dispersion of SWNTs should respond to the targeted usage of the nano-reinforcement. Individualization of the nanoparticles, so the particles are in contact with the matrix only, might be desirable when nanoscale properties are to be present in the final product. Conversely, slight contact between the nanoparticles is needed when the percolation phenomena through the entire domain are needed. In both cases, the interaction with the host polymer must be controlled. At the microscale, the production of nanocomposite structures must allow a control over the orientation of high aspect-ratio nanoparticles such as SWNTs. The arrangement of the nanocomposite microscale structures in 3D permits the localization and orientation of the nano-reinforcement in a macroscale product.

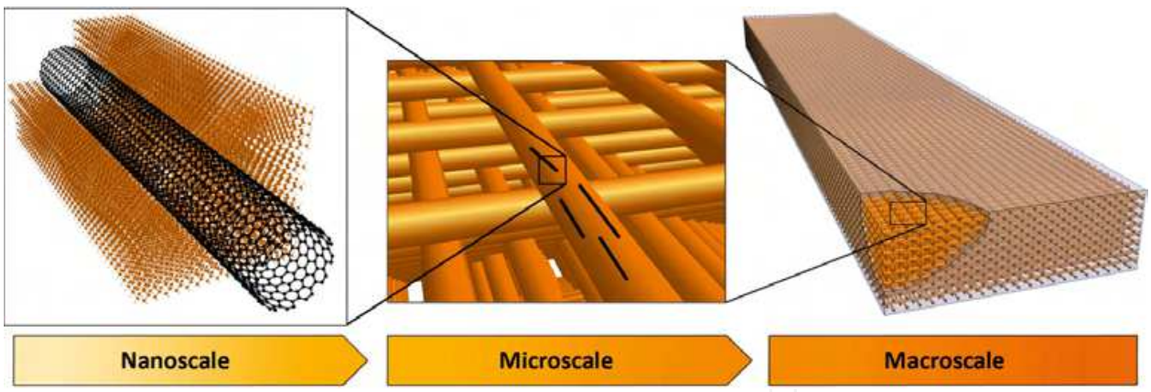

Fig. 1. Nano, micro and macro scales have to be considered for the successful manufacturing of a SWNT/Polymer nanocomposite.

3. Nanoscale

The nanoscale poses important manufacturing challenges such as the dispersion of the nanoparticles and the close interaction of the nanoparticles with the host polymer matrix (Byrne & Guin'Ko, 2010). In a dispersed state, the distance between particles in the matrix must be controlled to achieve the targeted properties. For mechanical reinforcement, every nanoparticle should be separated from each other to maximize the interface between the matrix and the nano-reinforcement, thus enhancing the available area for stress transfer to the nano-reinforcement. Aggregated nanoparticles are often responsible for underperformances. For example, carbon nanotube (CNT) aggregates in polymer nanocomposites can act as stress concentrators that trigger the fracture of the nanocomposite when submitted to moderate stress (Wong, Paramsothy et al., 2003). In carbon/magnetite nanocomposite produced by electro-spinning, the particle growth due to agglomeration during pyrolysis drastically reduces the paramagnetic property of the magnetite nanoparticle (Bayat, Yang et al., 2010). Conversely, contact between particles can be desirable to achieve an electrically percolated network in nanocomposites using CNTs. It has been observed that polymer coating around CNTs can lower the electrical conductivity of a nanocomposite due to the separation of the CNTs (Kilbride, Coleman et al., 2002).

Several studies theorized the quantity of particles that can be added to a polymer while keeping the continuity of the matrix phase (Coleman, Khan et al., 2006; Sandler, Pegel et al., 2004). The maximum concentration of SWNTs that can be added to a polymer without having discontinuities in the polymer phase was calculated using a hexagonal-packed array of aligned SWNTs and an interface zone of 5 nm. The maximum volume/volume (vol%) concentration was calculated at 1 vol%. Equation 1 can be used to understand this conclusion.

$$V_{f,\max} = \frac{\pi r^2}{2\sqrt{3}(1+r)^2} \quad with\ r = \frac{d}{c} \tag{1}$$

The maximum volume concentration ($V_{f,max}$) of cylindrical particles in a hexagonal packed arrangement is expressed as a function of the ratio (r) of the diameter of the cylinders (d) over the separation distance (c) between them. Figure 2 plots this relation and two examples are given: (1) the ratio of 0.12 for SWNTs of 1.2 nm diameter and a separation distance of 10

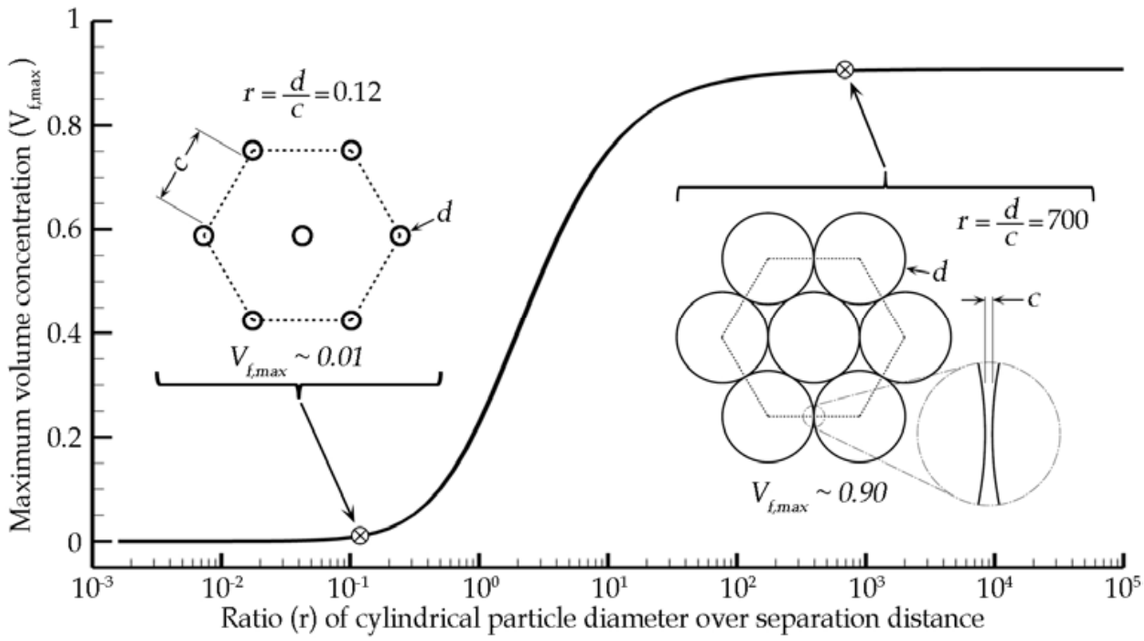

Fig. 2. Relation between the maximum volume concentration of cylindrical particles in hexagonal packing and the ratio (r) of the diameter (d) over the separation distance (c). Two examples are given for ratios of 0.12 and 700.

nm, which gives a maximum concentration of ~ 1 vol%; and (2) the ratio of 700 for carbon fibers of 7 μm with also a separation distance of 10 nanometers, which gives maximum concentration of ~ 90 vol%.

The interface zone is a certain thickness around nanoparticles where the polymer conformation is influenced by the nanoparticle. The value of the polymer radius of gyration is commonly employed to gage this distance. The radius of gyration of a polymer is the quadratic average of the distance between every monomer of the chain and the polymer mass center (Bicerano, 2002). It generally varies from 3 to 30 nm (Winey & Vaia, 2007). Using simulations, it has been shown that the surface of the nanoparticle provides a preferential orientation for the polymers also for a distance equal to the radius of gyration of the polymer (Starr, Schrder et al., 2002). However, special polymer conformation might as well exist in the case of higher strength or longer ranged interaction between the polymer and the nanoparticle. For example, several polymers having aromatic cycles can adopt a wrapping configuration around carbon nanotubes. This configuration has been observed with polyaniline (Sainz, Benito et al., 2005) and polyvinyl pyrolidone (O'Connell, Boul et al., 2001).

Moreover, nanoparticles, i.e. particles with at least one dimension in the order of the nanometer, possess a large area available for interaction with the host matrix compared to traditional composite reinforcements due to their high surface/volume ratio. For small diameter nanoparticles, the interface-affected volume might be larger than the volume of all the dispersed nanoparticles (Winey & Vaia, 2007). This interaction volume with the polymer can be tailored using covalent functionalization. For example, heating CNTs in inorganic acids (sulfuric and nitric) oxidize the CNTs mainly from the ends, grafting carboxylic groups. Such carboxylic groups may interact with the matrix to improve the stress transfer in mechanical applications. This carboxylic group is often used to further functionalize the CNTs by covalently attaching DNA (Baker, Cai et al., 2002) or ionically attaching

octadecylamine (Chen, Rao et al., 2001), for example. However, the chemical modification of the nanoparticle has to be done carefully to prevent the creation of defects that would lower the mechanical properties or change the electronic signature. Frankland *et al.* simulated a SWNT in a polyethylene matrix having a low density (< 1%) of covalent bounds between the matrix and the SWNT sidewalls. This configuration contributed to an augmentation of one order of magnitude of the shear stress transfer between the polymer and the SWNT without lowering significantly the tensile strength of the SWNT. However, the mechanical properties of the modified SWNT significantly dropped when 10% of the carbon atoms where modified (Frankland, Caglar et al., 2002). Moreover, extensive modification of the SWNT sidewall may destroy the delocalized π-electron system responsible for their electrical conductivity (Choi & Ihm, 1999).

Another approach is the usage of non-covalent functionalization of the carbon nanotube. The molecules used to perform this functionalization should have two functional ends: one that will preferably interact with the nanoparticle and another one that will interact with the host polymer matrix. Surfactants such as the sodium dodecyl sulfate, sodium dodecylbenzene sulfonate, or Triton X-100 are efficient to help the dispersion of carbon nanotubes in water (Islam, Rojas et al., 2003; Jiang, Gao et al., 2003). These molecules have a hydrophobic extremity that interacts with the CNT and a hydrophilic extremity that helps the dispersion in polar mediums like water. As stated previously, polymers can also wrap around CNTs. The wrapping process is attributed to the thermodynamic forces that tend to eliminate the hydrophobic interface between the CNT and the water (O'Connell, Boul et al., 2001). However, these wrapping techniques are not easily transferable to non-polar solutions such as the organic polymer matrices. Other successful non-covalent functionalizations are performed with molecules having polycyclic aromatic rings such as pyrenes (Chen, Zhang et al., 2001) and porphyrins (Satake, Miyajima et al., 2005). These groups can interact strongly with graphitic basal plane through π-π interactions.

Nanoscale dispersion is of paramount importance to benefit from the nanoparticle mechanical properties in a polymer nanocomposite. Nanoparticles have a tendency to agglomerate because, at such a small scale, the van der Waals forces are significant. This type of interaction comes from the deformation of the electron cloud around the atom, which creates an instant polarity that can be attracted by a nearby atom. In any case, a proper modification of the nanoparticle surface through covalent or non-covalent functionalization will prevent the re-agglomeration of the particles through steric or electrostatic forces.

Moreover, nanoparticles such as CNTs may have irregular shapes and, therefore, can be aggregated in their as-synthesized form. These aggregates greatly reduce the aspect-ratio of the nanoparticle or the available surface for interaction with the polymer (Thostenson & Chou, 2002). In this case, it might be difficult to achieve a nanoscale dispersion throughout the matrix (Stoeffler, Perrin-Sarazin et al., 2010).

Polymer nanocomposite with high aspect ratio nanoparticles can be highly viscous. Thus, the ultrasonic or mechanical mixing operations might generate undesirable heat, especially when integrating the nanoparticles to a thermoset polymer with a cross-linking reaction accelerated by temperature. The usage of a proper solvent is then favorable to reduce the viscosity during the integration into the matrix. Solvent-based processing also prevents the emission of air-born particles that might cause respiratory problems. An appropriate solvent must be able to both maintain the nanoparticles in suspension and dissolve the polymer. For CNT nanocomposites, tetrahydrofuran or toluene has been employed with polystryrene

(Thostenson & Chou, 2002; Wong, Paramsothy et al., 2003), dimethylformamide with poly-methyl methacrylate (Haggenmueller, Gommans et al., 2000), and chloroform with epoxy (Xu, Thwe et al., 2002). The nanocomposite is then recovered by evaporating the solvent in a vacuum oven or simply under a fume hood.

Ultrasonication is a common treatment employed to disperse nanoparticles in solvents and matrices. However, this technique does not individualize the CNTs and might just provide a good dispersion at the microscale. Also, re-agglomeration of CNTs have been observed when the ultrasonic treatment is stopped (Haggenmueller, Gommans et al., 2000).

Fluidic shear forces can help the dispersion of CNTs in a polymer matrix. Several types of mechanical mixers and homogenizers provide these forces. For example, the three-roll mill is composed of three cylinders rotating at different speeds and opposite directions. When the material passes through the small gap between to counter-rotating cylinders, the extreme shear forces generated are strong enough to disperse the nanoparticles at the nanoscale level (Gojny, Wichmann et al., 2004). When a thermoplastic polymer matrix is used, the fluidic shear forces in the extruder can help the dispersion of the nanoparticles. The shear forces can also come from the manufacturing process of the nanocomposite. For example, electro-spinning is a process in which a fiber is ejected from a spinneret with the help of a voltage applied between the spinneret and the substrate. The extreme shear forces involved during the ejection of the fiber have been considered responsible for the exfoliation of CNTs from their bundled nature (Ayutsede, Gandhi et al., 2006).

4. Microscale

The arrangement of nanocomposite material in structures typically at the micron to several hundred micron range offers several advantages. First, the material needed is reduced when the cost is an issue. In addition, the microstructures manufacturing techniques allow a better control on the nanoparticle disposition due to their microscale confinement. For example, high aspect ratio nanoparticles, such as CNTs, can align themselves along the flow direction with the help of the high shear achievable in small-scale manufacturing. Several techniques are used to produce nanocomposite at the microscale.

Microinjection molding (MIM) is an emerging method to manufacture microscale devices from polymer nanocomposites (Huang, Chen et al., 2006). Polycarbonate and multi-walled carbon nanotube (MWNT) nanocomposite microscale dog bone samples were manufactured by MIM. The high shear flow in the cavity while molding resulted in the alignment of the MWNTs along the flow direction (Abbasi, Carreau et al., 2010).

The process of fiber production, i.e. the “spinning”, works by forcing a viscous material through a small orifice, called a «spinneret». There are several variations of this process and each of them rely on specific viscoelastic properties of the spun material (Katayama & Tsuji, 1994).

The “melt spinning” is the most common method of producing fibers and has been used to produce CNT nanocomposite in thermoplastic matrices. After the integration of the nanoparticle in the polymer, the nanocomposite is extruded through a small orifice in a die, and the produced fiber is allowed to cool. During spinning, the fiber can be drawn. This will provide an extensional flow that orients the polymer molecules along the fiber direction. Several studies showed the alignment of CNTs along the flow direction and the positive effect on the mechanical properties of the fiber. (Sandler, Pegel et al., 2004; Thostenson & Chou, 2002).

"Solution spinning" was also used to produce carbon-nanotube fibers. This process extrudes a solution of nanocomposite in a non-solvent (Tsurumi, 1994). When the material is in contact with the non-solvent, a coagulation of the material occurs to form a fiber that can be collected. MWNT/polyvinyl alcohol (PVA) fibers were produced by solution spinning of water-based MWNT dispersion in an aqueous solution of PVA. The contact between the two solutions induced a polymer bridging coagulation of the MWNTs (Miaudet, Bartholome et al., 2007).

"Gel spinning" has been developed for the production of ultra-high molecular weight polyethylene fibers having ultra-high strength. The material has first to be treated to form a gel-like state that can be spun. This technique allows a superior control onto the molecular chains arrangement to produce a defect-free highly crystalline polymer fiber. Gel-spinning has also been used to produce SWNT/PVA nanocomposite fibers. The high alignment of the nano-reinforcement along the fiber axis improved the mechanical properties compared with pure PVA fibers (Minus, Chae et al., 2009).

Electro-spinning is another method widely used to produce nanocomposite fibers. In this method, the driving force for the spinning of the fiber is a voltage applied between the spinneret and the substrate. Highly charged polymer is ejected from the spinneret towards the substrate in the form of a fiber. The diameter of the produced fibers is typically in the range of 50 to 800 nm. SWNT reinforced polylactic acid and polyacrilonitrile nano-fibers have been produced using electro-spinning (Ko, Gogotsi et al., 2003).

5. Macroscale

Different techniques exist to manufacture nanocomposite products at the macroscale. A polymer nanocomposite can be simply molded in a shape before hardening either by cooling or by the effect of curing reaction. This relatively simple technique could find applications in traditional fiber reinforced composites by modifying the matrix-dominated properties. While the micro-fibers (e.g., glass, carbon, Kevlar) still serve as the main structural reinforcement, the nanoparticle enhanced polymer matrix could provide better fracture toughness and thermal stability, for example. More precisely, electrically conductive CNT/polymer matrix could give other functionalities to the composite such as electrostatic discharge protection, electromagnetic shielding and even strain and damage sensing (Thostenson & Chou, 2006). Although molding techniques are simple, they do not offer the possibility of controlling the position and orientation of the nanoparticles locally. Hence, it is challenging to position the nanoparticles where they are needed in a macroscopic product. Moreover, high-aspect ratio nanoparticles cannot be oriented along different directions corresponding to design requirements.

If the nanocomposite is manufactured in the form of continuous micro-fibers, weaving and braiding techniques can be used to dispose the nanocomposite in 3D. However textile-processing methods are labor-intensive and manufacture structures in repeating units only. Nanocomposite fibers produced by electro-spinning are usually randomly deposited on a substrate producing non-woven mats. Oriented electro-spun fiber layers can be assembled by employing a special collector electrode arrangement (Li & Xia, 2004). The obtained uni- or multi-directional fiber films can provide a control of the orientation of nanoparticles in 1D or 2D. Techniques that produce films – that is, solvent casting (Xu, Zhang et al., 2006), spin coating (Xu, Thwe et al., 2002), layer-by-layer (Mamedov, Kotov

et al., 2002), extrusion and stretching (Thostenson & Chou, 2002), or compression (Haggenmueller, Gommans et al., 2000) – are known to produce random alignment of CNTs in 2D or even alignment in 1D. Stereo-lithography can also be used to build 3D macroscale products from UV-curing polymers. A thin layer of nanocomposite is cured on the surface of a resin bath using localized UV exposure. Layers of material are successively hardened on top of each other to form a 3D structure. Stereo-lithography has been used to manufacture 3D structures with CNT nanocomposite (Varadan, Xie et al., 2001), or ceramic nanoparticle nanocomposites (Varadan & Varadan, 2001). However, this technique cannot orient axisymmetric nanoparticles during manufacturing because no force is applied on the particles randomly dispersed in the resin bath. Also, due to the layer-by-layer curing, curved surfaces on the vertical plane will be formed by a succession of discrete right angles.

Microfibers can be assembled in structures using the direct-write fabrication method. This manufacturing technique consists of the motion of an extrusion micro-nozzle that generates defined patterns in 3D with material filaments (Lewis & Gratson, 2004). The deposited material, generally called "ink", is extruded and allowed to lie on a substrate along a defined pattern. Then, the extrusion nozzle is raised by an increment and other filaments can be deposited on the previous layer. The stacking of the filaments produces a 3D structure. This method is relatively simple and the resolution of products can be down to the micrometer range (Gratson, Garcia-Santamaria et al., 2006). During direct writing, the displacement speed of the extrusion device should match the linear extrusion rate of material from the nozzle. However, a slightly higher displacement speed will stretch the filament, thereby providing an extensional flow, enhancing the alignment of the nanoparticles.

The ink must have tailored viscoelastic properties to enable 3D manufacturing. That is, it must be fluid enough to be extruded through a micro-nozzle. Additionally, its rigidity must increase after extrusion to form a filament that can be deposited between support points. Several materials offer this type of behavior. Organic fugitive inks with superior stiffness have been used as self-supporting spanning filaments. This material also exhibited moderate shear yield stress to facilitate extrusion through a deposition nozzle. The development of this fugitive ink enable the direct-write manufacturing of filamentary scaffold structures having more than a hundred layers (Therriault, Shepherd et al., 2005). Spanning filaments of silver nanoparticle reinforced polyacrylic acid were deposited by direct-write between two electrodes with out-of-plane filament curvature (Ahn, Duoss et al., 2009). After material sintering, the filament insured the electrical connectivity between individual micro-solar cells of a solar panel. Figure 3 illustrates the deposition of filaments using the direct-write technique.

The various direct-write techniques have been limited mainly to supported structures in a layer-by-layer building sequence and straight spanning filaments between support points. This limitation comes from the fact that for shear-thinning inks, the ink rigidity increases at the same moment as the ink exits the extrusion nozzle, that is, when the shear strain applied to the material returns to a near zero value. Therefore, the extruded filament has the same rigidity from its extrusion point to the previous support point. Given these conditions, the application of a side force due to the extrusion nozzle changing direction results in a bending moment that reaches a maximum at the support point, hence creating a deflection of the whole deposited filament (see Figure 3b).

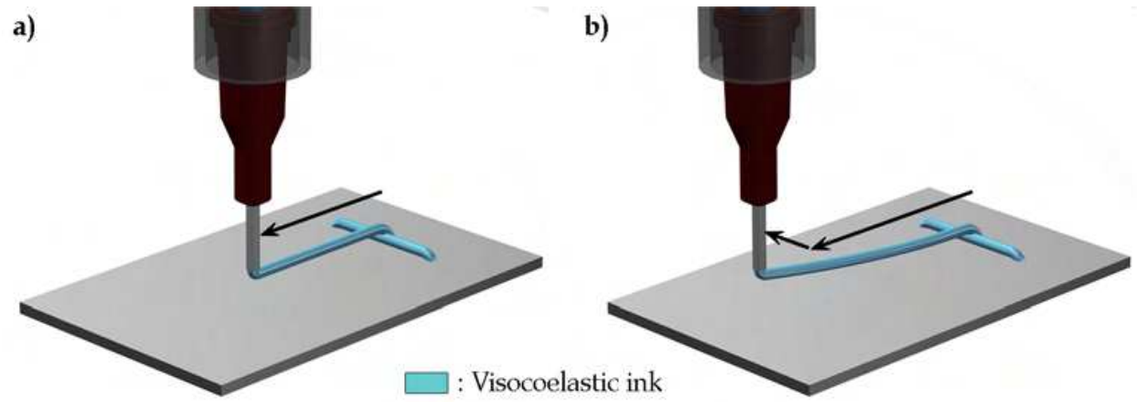

Fig. 3. Direct-write deposition of a viscoelastic filament: a) Extrusion of a filament having the same rigidity from the extrusion point to its anchoring point. b) Bending of the whole filament when the extrusion nozzle changes direction.

6. Multi-scale fabrication of SWNT/polyurethane nanocomposite structures

The following sections present an example of multi-scale manufacturing of nanocomposite structures using SWNTs and a UV-curable polyurethane. The challenges involved at the nano-, micro-, and macroscales are addressed step-by-step. First, the SWNTs are dispersed in the polyurethane using functionalization and shear mixing. Then, micro-fibers are deposited using the direct-write technique. Finally, two methods involving the direct-write assembly technique are employed to manufacture tridimensional nanocomposite structures.

6.1 Nanoscale: integration of SWNTs to a polyurethane polymer

A SWNT/polyurethane compound can be prepared according to the procedure schematized in Figure 4. Before integration to the polymer, a reflux of five hours in a nitric acid solution was used to treat the as-grown SWNTs. This treatment purified the as-grown material and also attached carboxylic chemical groups onto the nanotube sidewall (see Figure 4-1). The nanotube purity and covalent modification was verified by transmission electron microscope, Raman microscopy, thermo--gravimetric analysis, and X-ray photoelectron microscopy. A non-covalent modification was also performed by sonicating a specific amount of the purified SWNTs in a 0.1 mM solution of Zinc Protoporphyrin IX (ZnPP) in the dichloromethane (DCM) solvent (see Figure 4-2). As stated earlier, the porphyrin end of the ZnPP molecule have polycyclic aromatic hydrocarbon end that adhere to the nanotube sidewall through $\pi - \pi$ interaction. The other end of the molecule is composed of carboxylic groups, which offer possible interaction sites with the matrix.

A commercially available UV-curable polyurethane (NEA123MB, Norland Products) was then slowly added to the SWNT solution in DCM while stirring with a magnetic stirrer (see Figure 4-3 and 4-4). The polyurethane has –CONH- groups on the polymer backbone capable of interacting with the carboxylic groups on the covalently and non-covalently modified SWNTs (Sahoo, Jung et al., 2006). After evaporation of the DCM solvent (see Figure 4-5), the nanocomposite mixture was passed several times in a three-roll mixer mill where the gap between the rolls and the speed of the apron roll were controlled (Figure 4-6). Fumed silica nanoparticles were also added to increase the viscosity and to yield a shear-thinning behavior (Raghavan, Walls et al., 2000). The nanocomposite was slowly added to a

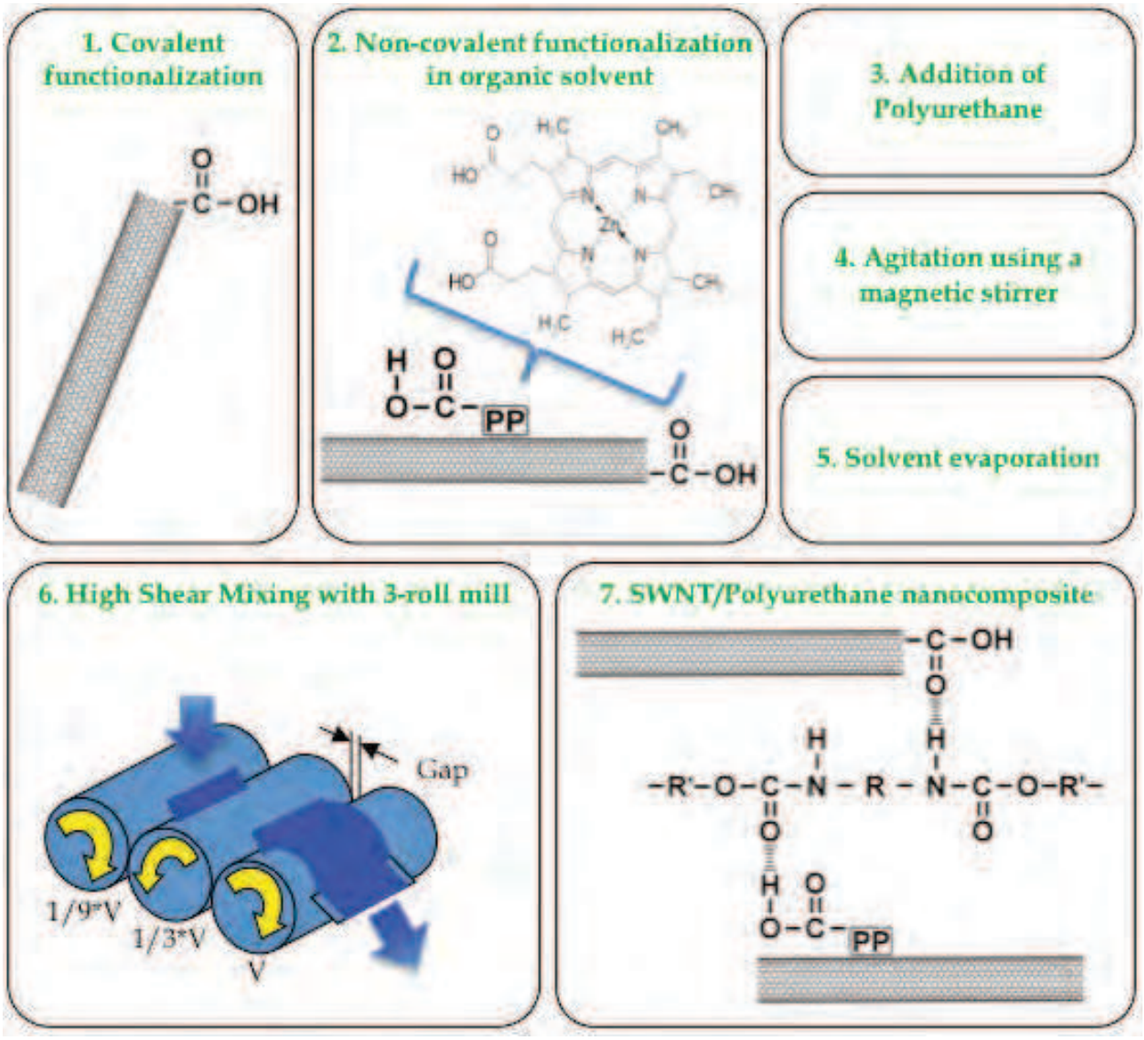

Fig. 4. Preparation steps for the integration of SWNTs to a polyurethane matrix

fumed silica nanoparticle solution in DCM while mixing. Finally, the nanocomposite was poured into syringe barrels, where the DCM solvent was fully evaporated. The whole procedure produced UV-curable nanocomposites containing 0.5 wt% of purified and functionalized SWNTs and 5 wt% of fumed silica (see complete experimental details in (Lebel, Aissa et al., 2009)).

Figure 5a shows the microscopic scale dispersion of the final nanocomposite. Dark spots, of average size of ~ 1.3 μm, are observed in the nanocomposite blend. These spots are believed to be aggregates of carbonaceous materials or SWNTs entangled around larger carbon particles. From the observation of the distribution of the visible dark spots, one can assume that the SWNTs, along with their associated agglomerates, were uniformly dispersed in the polyurethane matrix. However, it is difficult to ascertain that all the SWNTs are exfoliated and dispersed at the nanoscale level. Such distribution was also often obtained in other studies (Bose, Khare et al., 2010). This trend poses a serious question about the possibility of de-agglomeration of SWNT when they are aggregated or bundled in their as-grown form by traditional means. In case the raw material is highly aggregated, an ultra-centrifugation

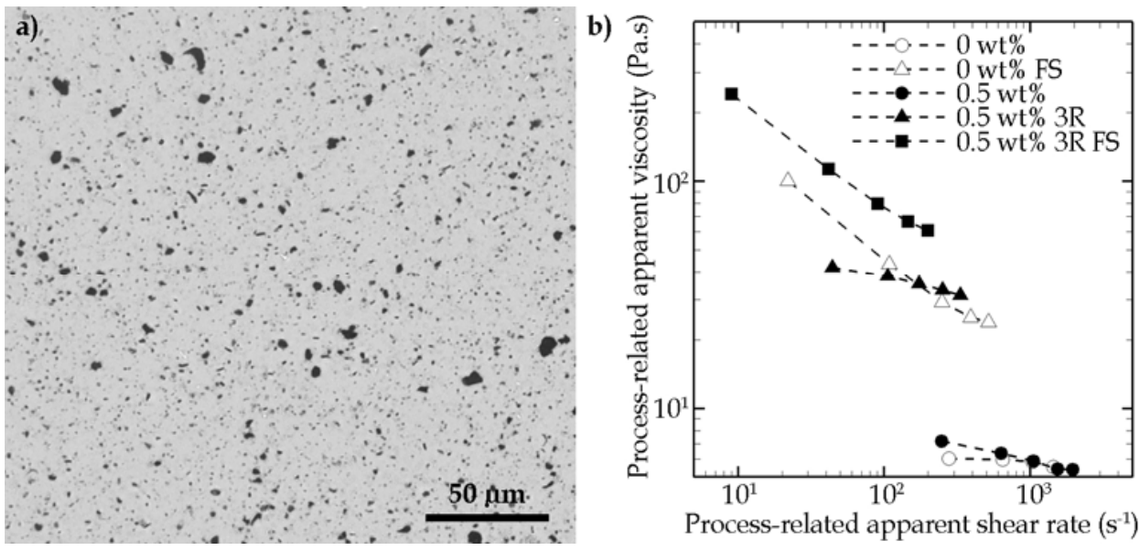

Fig. 5. a) Optical microscope image of SWNT/Polyurethane nanocomposite illustrating its dispersion at the microscale. b) Apparent viscosity measurements of the nanocomposite at different stages during the integration process.

procedure should be performed after the solubilization of the nanoparticle in the organic solvent with the aid of functionalization (see figure 4, between steps 2 and 3). Ultracentrifugation is a well-known technique to separate the SWNT material from the aggregates (Kim, Nepal et al., 2005) and can also be used to segregate SWNTs based on their electronic properties (Green & Hersam, 2007).

The apparent viscosity is a good indicator of the dispersion of the SWNTs. Well-dispersed SWNTs increase the viscosity and may create a shear thinning behavior. It has been observed that the shear-thinning behavior of a SWNT/polymer nanocomposite can be caused by a rheological percolation network that is created when the critical percolation concentration is reached (Du, Scogna et al., 2004). The latter is more sensitive to the aspect ratio (i.e. length over diameter) of the reinforcing nano-material rather than to its actual size (Balberg, Binenbaum et al., 1984).

Figure 5b shows the process-related viscosity at different shear rates measured by capillary viscometry at different steps during the integration procedure. The indication 0 wt% stands for pure polyurethane; 0.5 wt% stands for the polyurethane having a 0.5 wt% concentration of SWNTs; 0.5 wt% 3R stands for the nanocomposite mix after the three-roll mixing; and 0.5 wt% 3R FS stands for the nanocomposite after the addition of fumed silica. These results where compared with polyurethane also having a 5 wt% fumed silica charge (0 wt% FS). The process-related apparent viscosity (η) values were plotted on a log-log graph as a function of the shear rate ($\dot{\gamma}$) and fitted with a power-law fluid relationship according to the following equation:

$$\eta = m\dot{\gamma}^{(1-n)} \tag{2}$$

Table 1 lists the calculated values of the power-law indexes (n) as an indication of the viscosity behavior with respect to the strain rate. The sample 0 wt% has an index near 1 showing a Newtonian behavior, as the value of viscosity does not vary across the strain

rates investigated. The first mixing stage consisted of the incorporation of the SWNTs in the polyurethane resin. After the nanotube incorporation, a slight shear-thinning behavior was observed (0.5 wt%, $n \approx 0.85$) due to nanotubes that formed a viscosity-percolated network. After the three-roll mixing, a drastic viscosity increase was observed, indicating that the three-roll mill reduced the size of aggregates and successfully dispersed the added material. However, the calculated viscosity indexes after this mixing stage remained unchanged. Thus, it can be argued that the three-roll mixing step did not generate higher aspect-ratio entities (i.e., individual nanotubes). The incorporation of fumed silica particles further increased the viscosity and changed the rheological behavior, as indicated by the viscosity index reaching a value of 0.5. A similar response is observed at different intensities for the 0 wt%-FS, whose power-law index value is comparable. This effect is the result of a network formation of hydrogen bonded fumed silica particles that impart a gel-like rheological behavior to the mixture at rest. The apparent viscosity diminishes under the application of a moderate shear force destroying the weakly bounded network (Raghavan, Walls et al., 2000).

Sample	Viscosity index (n)
0 wt%	0.95
0 wt% FS	0.53
0.5 wt%	0.85
0.5 wt% 3R	0.86
0.5 wt% 3R FS	0.55

Table 1. Viscosity indexes of nanocomposite blends.

The preparation procedure resulted in two nanocomposite mixtures. The low viscosity nanocomposite, that is, the 0.5 wt% 3R, can be used in casting or molding situations, while the high viscosity nanocomposite, that is, the 0.5 wt% 3R FS, has a gel-like rheological behavior that is readily spinnable in the form of fibers.

6.2 Microscale: UV-assisted direct-write fabrication of nanocomposite fibers.

The UV-curable nanocomposite (0.5 wt% 3R FS) prepared according to the procedure in section 6.1 can be placed in a syringe barrel equipped with a micro-nozzle tip. Under the application pressure, the gel-like nanocomposite is extruded through the micro-nozzle to form a fiber. Also, the syringe barrel can be displaced in the 3D space using a micro-positioning robot. Then, using a UV source that follows the extrusion point, the material is cured right after extrusion to form a fiber that can span between two support points. Figure 6a describes the ultraviolet-assisted direct-write (UV-DW) fabrication of nanocomposite fibers. A fiber is extruded between two polymer pads by robotic displacement of an extrusion nozzle. The fiber is exposed right after extrusion to a UV-source to cure the nanocomposite. Figure 6b shows the actual fiber produced and Figure 6c shows the stress-strain curve measured using a dynamic mechanical analyzer while testing the nanocomposite (0.5 wt% 3R FS) and polyurethane (0 wt% FS) fibers under tensile loading.

The stress-strain curves shown in Figure 6c indicate a clear change in the mechanical behavior between the unloaded polyurethane fibers and the nanocomposite ones. The unloaded material (0 wt% FS) exhibits a non-linear response of the stress under strain and experiences a large elongation before rupture. In contrast, the nanocomposite (0.5 wt% 3R FS) response is rather elastic and linear until breakage, which is reached at rather shorter

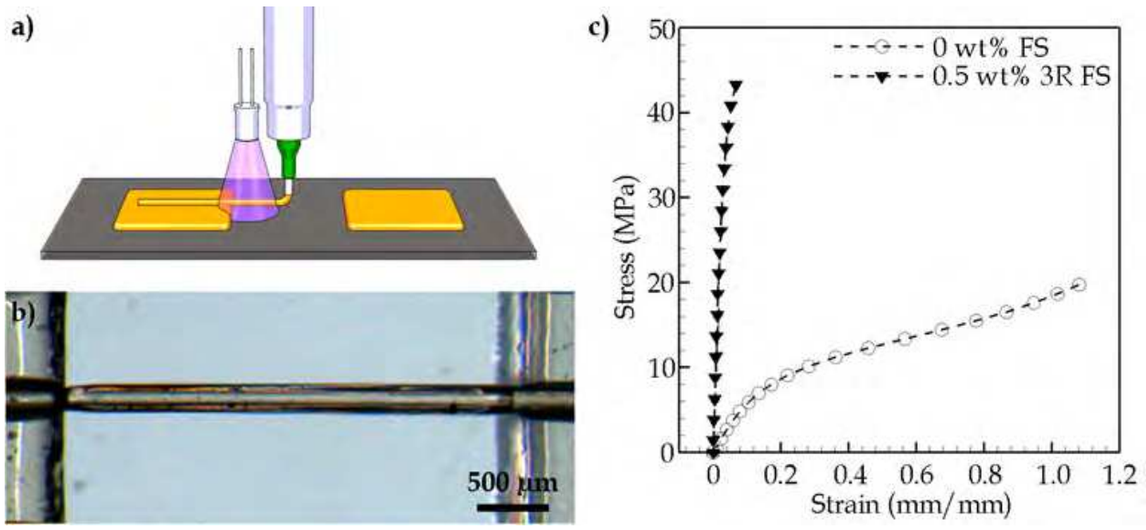

Fig. 6. Production of a SWNT/Polyurethane nanocomposite fiber by ultraviolet-assisted direct writing. a) The fiber is extruded using a moving micro-nozzle between two polymer pads. b) Optical microscope image of the produced fiber between two pads. c) Mechanical characterization of the nanocomposite fiber.

elongations. This radically different behavior in comparison with the unloaded polyurethane is attributed to the SWNTs incorporation and a significant stress transfer between the host matrix and the nano-reinforcement. The mechanical characterization of the microfibers revealed a significant increase in both the strength (by ~64%) and the stiffness (by more than 15 times). These mechanical enhancements were attributed to the presence of SWNT, and both the covalent and the non-covalent functionalizations of the SWNTs (Lebel, Aissa et al., 2009).

6.3 Macroscale: fabrication of 3D SWNT/polyurethane nanocomposite structures using direct-write techniques

The direct-write techniques offer the possibility of arranging fibers in three dimensions. Two approaches have been developed using the nanocomposite prepared according to the procedure in section 6.1. The low viscosity nanocomposite (0.5 wt% 3R) was used for the infiltration of 3D micro-fluidic networks. The more viscous and shear thinning nanocomposite (0.5 wt% 3R FS) was deposited in 3D using the UV-DW approach. The following sections briefly present these two approaches.

6.3.1 Nanocomposite infiltration in 3D microfluidic network

This approach permits the fabrication of a 3D-reinforced product through the directed and localized infiltration of SWNT/polymer nanocomposites into a 3D microfluidic network. These microfluidic networks are created using the flexible direct-write assembly method of organic fugitive ink. Figure 7 illustrates the manufacturing steps to manufacture nanocomposites beams by the microfluidic infiltration approach. The direct-write assembly method is first used to generate a scaffold of fugitive ink filaments (Figure 7a). The rigidity of this type of ink at room temperature is high enough to resist deformation when the filament is disposed between two support points. The filaments can also be layered without the collapse of the scaffold structure (Therriault, White et al., 2003). The architecture of the

scaffold can be tailored at will by controlling the number and orientation of filaments in every layer (Figure 7b). After completion of the deposition, an epoxy matrix is used to encapsulate the scaffold (Figure 7c). The resin is then allowed to harden around the fugitive ink filaments. Heat generation during curing reaction of the resin is kept to a minimum to prevent deformation of the fugitive ink scaffold. In the fourth step, the encapsulated ink filaments are heated to liquid state and then drained to obtain a 3D microfluidic network, which is reproducing the ink filament scaffold architecture (Figure 7d). In the fifth step, the microfluidic network is infiltrated with a SWNT/polymer nanocomposite fluid (Figure 7e). The final step is to cure the nanocomposite to obtain an epoxy beam reinforced by a 3D network of nanocomposite fibers (Figure 7f). This technique allows the designer to place nanocomposite filaments were they are needed in a macroscopic product. Moreover, at the structural level, stress concentration is low due to the circular cross-section of the produced microfluidic channels.

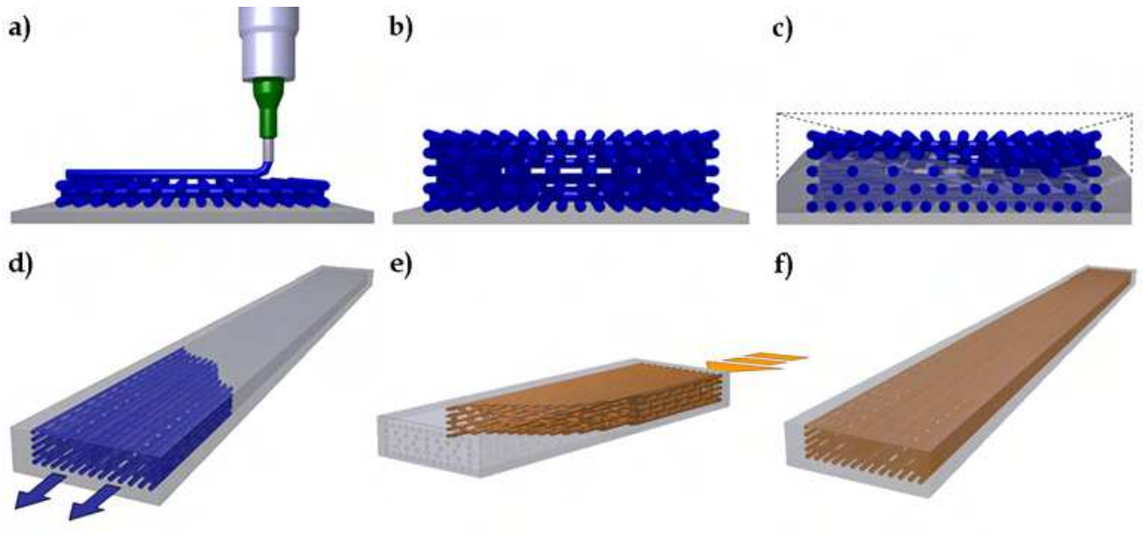

Fig. 7. Production of a macroscale nanocomposite structure by the infiltration of a microfluidic network.

By using the technique depicted in Figure 7, nanocomposite-reinforced rectangular beams were manufactured to provide good bending rigidity. Flexural mechanical solicitation generates an axial stress distribution that linearly increases from the neutral mid-plane until reaching a maximum value at the outer surfaces. Figure 8a shows the as-produced beam reinforced by a nanocomposite micro-fiber skeleton. Figure 8b shows a top view image of the beam where perpendicular (in the lateral direction) microfluidic channels were required to support and interconnect the different levels of axial fibers to facilitate the complete filling of the 3D microstructure. Figure 8c shows a beam cross-section where the number of axial reinforcing infiltrated microfibers was increased in higher stress regions of the cross-section. Dynamic mechanical analysis in bending showed an increase of 12.5% in the storage modulus at temperatures below 35°C compared to the neat resin infiltrated beams (Lebel, Aissa et al., 2009). This technique can be compared to microinjection molding with the particularity that both the mold and the injected structure are part of the same product. No particular rheological behavior is needed as long as the viscosity is sufficiently low. High viscosity nanocomposite need high injection pressure that could damage the microfluidic network during nanocomposite injection.

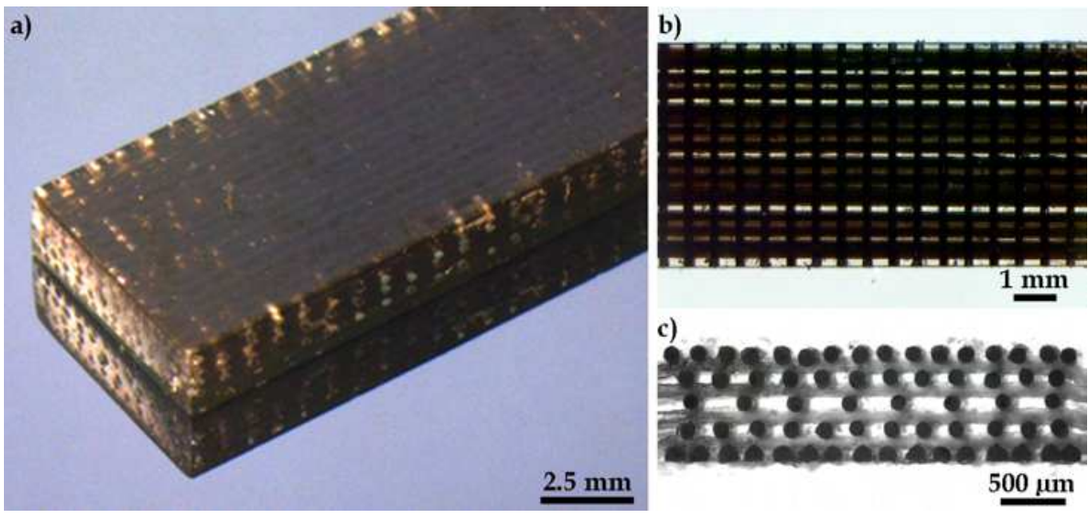

Fig. 8. a) Nanocomposite reinforced beam. b) Top view of the beam showing the injected nanocomposite fibers. c) Cross-section of the beam. The black circles are the axial fiber cross-sections.

6.3.2 3D fabrication by ultraviolet-assisted direct-write

As previously seen, DW techniques are limited to deposition of straight or simply curved filaments. In order to create a curved shape by changing the moving path of the extrusion nozzle, another increase in rigidity has to occur slightly distanced from the extrusion point. As a result, the filament bending will occur at the transition zone between to the low bending rigidity of the newly deposited material and the higher bending rigidity of the cured spanning filament previously deposited. This principle is illustrated in Figure 9, where the filament bends before and during cure of the material under exposure to UV.

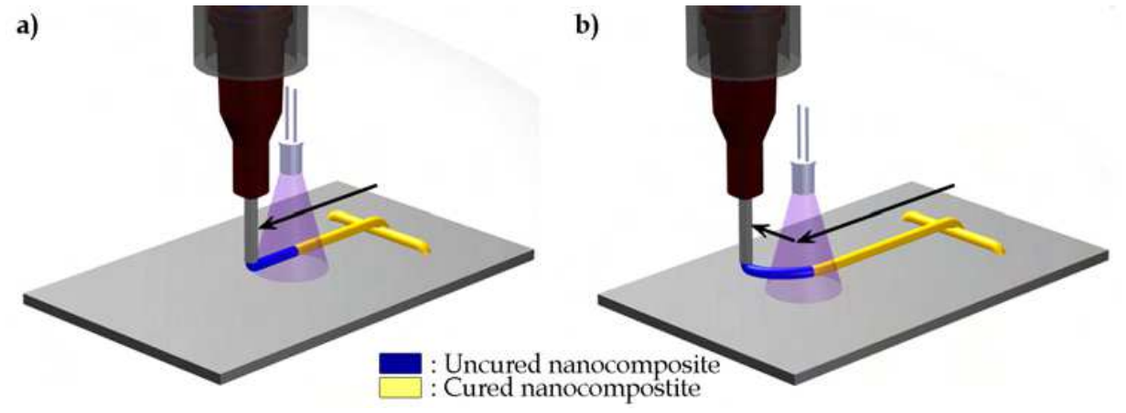

Fig. 9. Concept of ultraviolet-assisted direct-write technique a) Deposition and curing of a nanocomposite filament using an UV source following the extrusion nozzle. b) Filament curvature initiated at the curing transition zone, following the extrusion nozzle path.

The ultraviolet-assisted direct-write method extends the manufacturing space for nanocomposite structures and opens up new prospects for nanocomposite devices in 3D. For successful fabrication using the UV-DW technique, the nanocomposite curing speed under radiation must match closely or be faster than the moving speed of the extrusion device.

Moreover, the distance between the UV radiation exposure and the filament extrusion point has to be carefully calibrated. If the curing reaction is triggered in the extrusion nozzle, there is a risk of clogging. If the curing reaction is triggered far from the extrusion point, the nanocomposite filament will not reproduce the moving path of the extrusion point. The ability to cure the nanocomposite along a certain extrusion path allows the designer to create curve-shaped structures in space such as the ones presented in Figure 10.

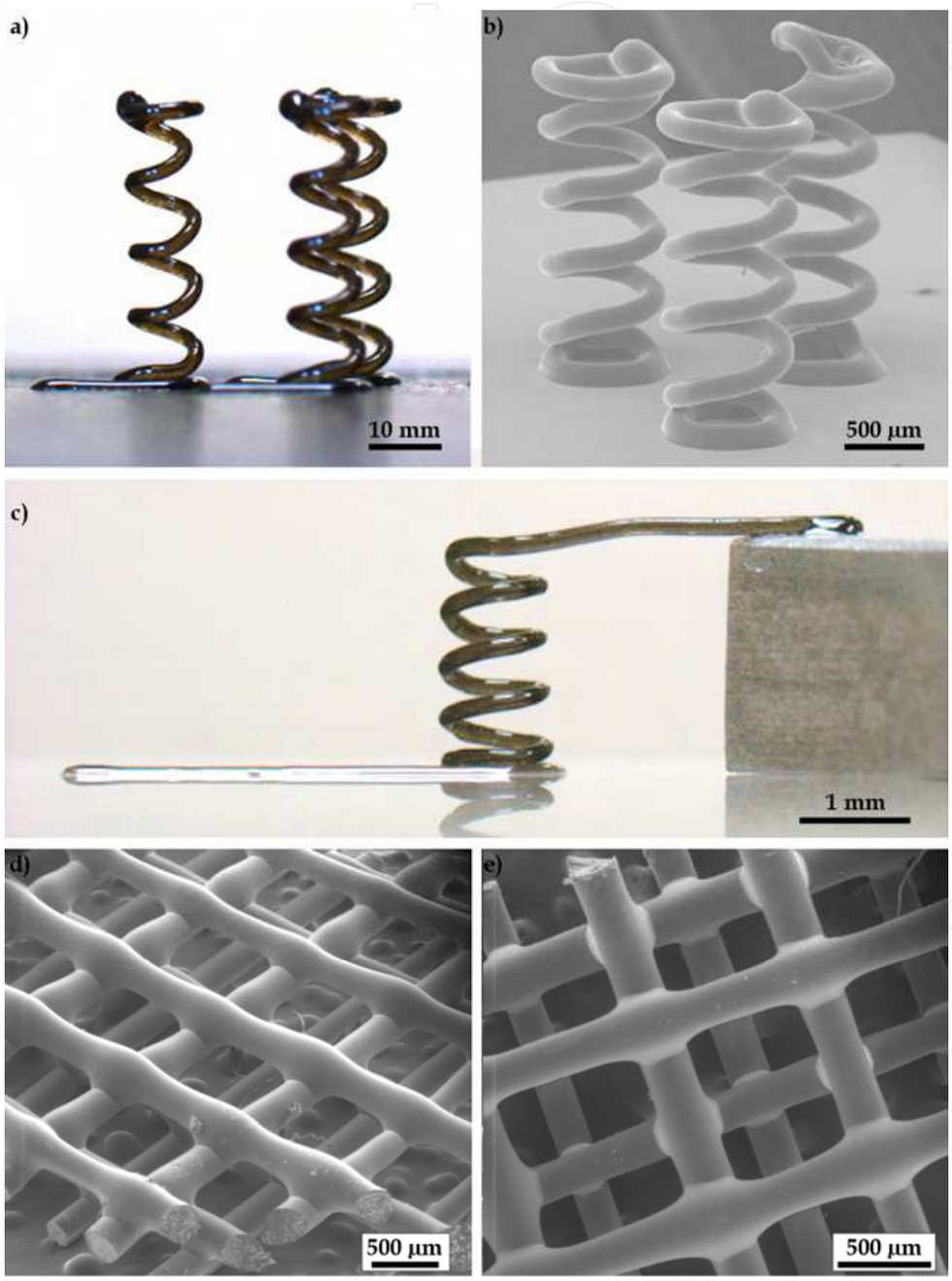

Fig. 10. Several nanocomposite structures manufactured by UV-DW: a-b) Coiled micro-spring network. c) Coiled wire between a substrate and an electrode. d-e) Scaffold structure.

Nanocomposite spring network composed of three micro-coils (Figure 10a) were fabricated using the UV-DW technique. Each of the springs had a filament diameter of ~ 150 μm, a coil diameter of ~ 1 mm and a height of ~ 4 mm. The networks were mechanically tested under compression and showed a rigidity of ~ 11.5 mN/mm. A smaller network of coils was also fabricated (Figure 10b). In this case, the coils had a ~100 μm diameter filament and a ~ 500 μm coil diameter. A micro-coil using a ~ 200 μm nanocomposite filament was also deposited to bridge the gap of ~2.1 mm between two uneven substrates (Figure 10c). This demonstration of an organic inductance device had a 10^{-6} S/cm electrical conductivity (Lebel, Aissa et al., 2009). Nanocomposite scaffold structures (Figure 10d-e) were also deposited using the UV-DW technique. The filaments were deposited in a layer-by layer sequence with the orientation of the filament being perpendicular from a layer to the other. The filament diameter were ~ 200 μm and the spacing between filaments among the same layer was ~ 1 mm.

7. Conclusion

The fabrication of high-performance nanocomposite materials and complex 3D structures must overcome the different challenges at the nano-, micro-, and macroscale. Dispersion and interaction with the polymer matrix are of paramount importance at the nanoscale. The microscale manufacturing techniques should provide a control over the orientation of high aspect-ratio nanoparticles such as carbon nanotubes. Finally, proper assembly technique of microstructures should be developed to create functional devices at the macroscale. The manufacturing techniques explained in this chapter, i.e. the infiltration of 3D microfluidic networks and UV-assisted direct writing, represent new avenues for the creation of 3D reinforced micro- and macrostructures that could find applications in organic electronics, polymer-based MEMS, sensors, tissue engineering scaffolds and aerospace structures.

8. References

Abbasi, S.; Carreau, P. J. & Derdouri, A. (2010). Flow induced orientation of multiwalled carbon nanotubes in polycarbonate nanocomposites: Rheology, conductivity and mechanical properties. *Polymer*, Vol. 51, No. 4, (February 2010) 922-935, 0032-3861

Ahn, B. Y.; Duoss, E. B.; Motala, M. J.; Guo, X.; Park, S.-I.; Xiong, Y.; Yoon, J.; Nuzzo, R. G.; Rogers, J. A. & Lewis, J. A. (2009). Omnidirectional Printing of Flexible, Stretchable, and Spanning Silver Microelectrodes. *Science*, Vol. 323, No. 5921, (March 2009) 1590-1593, 0036-8075

Ayutsede, J.; Gandhi, M.; Sukiraga, S.; Ye, H.; Hsu, C.-M.; Gogotsi, Y. & Ko, F. (2006). Carbon nanotube reinforced Bombyx mori silk nanofibers by the electrospinning process. *Biomacromolecules*, Vol. 7, No. 1, (January 2006) 208-214, 1525-7797

Baker, S. E.; Cai, W.; Lasseter, T. L.; Weidkamp, K. P. & Hamers, R. J. (2002). Covalently Bonded Adducts of Deoxyribonucleic Acid (DNA) Oligonucleotides with Single-Wall Carbon Nanotubes: Synthesis and Hybridization. *Nano Letters*, Vol. 2, No. 12, (October 2002) 1413-1417, 1530-6984

Balberg, I.; Binenbaum, N. & Wagner, N. (1984). Percolation thresholds in the three-dimensional sticks system. *Physical Review Letters*, Vol. 52, No. 17, (April 1984) 1465-8, 0031-9007

Bayat, M.; Yang, H. & Ko, F. (2010). Structure and Properties of Superparamagnetic Composite Nanofiber, *Proceedings of 8th Joint Canada-Japan Workshop on Composites*, Montreal, Canada, July 26-29, 2010, DEStech Publications Inc, In press

Bicerano, J. (2002). *Prediction of polymer properties*, Marcel Dekker, 0-8247-0821-0, New York

Bose, S.; Khare, R. A. & Moldenaers, P. (2010). Assessing the strengths and weaknesses of various types of pre-treatments of carbon nanotubes on the properties of polymer/carbon nanotubes composites: A critical review. *Polymer*, Vol. 51, No. 5, (March 2010) 975-993, 0032-3861

Byrne, M. T. & Guin'Ko, Y. K. (2010). Recent advances in research on carbon nanotube - polymer composites. *Advanced Materials*, Vol. 22, No. 15, (April 2010) 1672-1688, 0935-9648

Chen, J.; Rao, A. M.; Lyuksyutov, S.; Itkis, M. E.; Hamon, M. A.; Hu, H.; Cohn, R. W.; Eklund, P. C.; Colbert, D. T.; Smalley, R. E. & Haddon, R. C. (2001). Dissolution of full-length single-walled carbon nanotubes. *Journal of Physical Chemistry B*, Vol. 105, No. 13, (April 2010) 2525-2528, 1089-5647

Chen, R. J.; Zhang, Y.; Wang, D. & Dai, H. (2001). Noncovalent sidewall functionalization of single-walled carbon nanotubes for protein immobilization. *Journal of the American Chemical Society*, Vol. 123, No. 16, (April 2001) 3838-3839, 0002-7863

Choi, H. J. & Ihm, J. (1999). Exact solutions to the tight-binding model for the conductance of carbon nanotubes. *Solid State Communications*, Vol. 111, No. 7, (July 1999) 385-90, 0038-1098

Coleman, J. N.; Khan, U.; Blau, W. J. & Gun'ko, Y. K. (2006). Small but strong: A review of the mechanical properties of carbon nanotube-polymer composites. *Carbon*, Vol. 44, No. 9, (August 2010) 1624-1652, 0008-6223

Du, F.; Scogna, R. C.; Zhou, W.; Brand, S.; Fischer, J. E. & Winey, K. I. (2004). Nanotube networks in polymer nanocomposites: rheology and electrical conductivity. *Macromolecules*, Vol. 37, No. 24, (November 2004) 9048-9055, 0024-9297

Frankland, S. J. V.; Caglar, A.; Brenner, D. W. & Griebel, M. (2002). Molecular simulation of the influence of chemical cross-links on the shear strength of carbon nanotube-polymer interfaces. *Journal of Physical Chemistry B*, Vol. 106, No. 12, (March 2002) 3046-3048, 1089-5647

Gojny, F. H.; Wichmann, M. H. G.; Kopke, U.; Fiedler, B. & Schulte, K. (2004). Carbon nanotube-reinforced epoxy-composites: Enhanced stiffness and fracture toughness at low nanotube content. *Composites Science and Technology*, Vol. 64, No. 15 SPEC ISS, (November 2004) 2363-2371, 0266-3538

Gratson, G. M.; Garcia-Santamaria, F.; Lousse, V.; Xu, M.; Fan, S.; Lewis, J. A. & Braun, P. V. (2006). Direct-write assembly of three-dimensional photonic crystals: Conversion of polymer scaffolds to silicon hollow-woodpile structures. *Advanced Materials*, Vol. 18, No. 4, (Febuary 2006) 461-465, 0935-9648

Green, A. A. & Hersam, M. C. (2007). Ultracentrifugation of single-walled nanotubes. *Materials Today*, Vol. 10, No. 12, (December 2007) 59-60, 1369-7021

Haggenmueller, R.; Gommans, H. H.; Rinzler, A. G.; Fischer, J. E. & Winey, K. I. (2000). Aligned Single-Wall Carbon Nanotubes in Composites by Melt Processing Methods. *Chemical Physics Letters*, Vol. 330, No. 3-4, (November 2000) 219-225, 0009-2614

Huang, C. K.; Chen, S. W. & Wei, W. C. J. (2006). Processing and property improvement of polymeric composites with added ZnO nanoparticles through microinjection molding. *Journal of Applied Polymer Science*, Vol. 102, No. 6, (December 2006) 6009-6016, 0021-8995

Islam, M. F.; Rojas, E.; Bergey, D. M.; Johnson, A. T. & Yodh, A. G. (2003). High Weight Fraction Surfactant Solubilization of Single-Wall Carbon Nanotubes in Water. *Nano Letters*, Vol. 3, No. 2, (February 2003) 269-273, 1530-6984

Jiang, L.; Gao, L. & Sun, J. (2003). Production of aqueous colloidal dispersions of carbon nanotubes. *Journal of Colloid and Interface Science*, Vol. 260, No. 1, (April 2003) 89-94, 0021-9797

Katayama, K.-i. & Tsuji, M. (1994). Fundamentals of spinning. In: *Advanced fiber spinning technology*. Nakajima, T., Kajiwara, K. & McIntyre , J. E. (Ed.). 1-24. Woodhead Publishing Ltd., 1 85573 182 7, Cambridge, England

Kilbride, B. E.; Coleman, J. N.; Fraysse, J.; Fournet, P.; Cadek, M.; Drury, A.; Hutzler, S.; Roth, S. & Blau, W. J. (2002). Experimental observation of scaling laws for alternating current and direct current conductivity in polymer-carbon nanotube composite thin films. *Journal of Applied Physics*, Vol. 92, No. 7, (October 2002) 4024-30, 0021-8979

Kim, D. S.; Nepal, D. & Geckeler, K. E. (2005). Individualization of single-walled carbon nanotubes: Is the solvent important? *Small*, Vol. 1, No. 11, (November 2005) 1117-1124, 1613-6810

Ko, F.; Gogotsi, Y.; Ali, A.; Naguib, N.; Ye, H.; Yang, G.; Li, C. & Willis, P. (2003). Electrospinning of continuous carbon nanotube-filled nanofiber yarns. *Advanced Materials*, Vol. 15, No. 14, (July 2003) 1161-1165, 0935-9648

Lebel, L. L.; Aissa, B.; El Khakani, M. A. & Therriault, D. (2009). Ultraviolet-assisted direct-write fabrication of carbon nanotube/polymer nanocomposite microcoils. *Advanced Materials*, Vol. 22, No. 5, (February 2010) 592-596, 0935-9648

Lebel, L. L.; Aissa, B.; Khakani, M. A. E. & Therriault, D. (2009). Preparation and mechanical characterization of laser ablated single-walled carbon-nanotubes/polyurethane nanocomposite microbeams. *Composites Science and Technology*, Vol. 70, No. 3, (March 2010) 518-524, 0266-3538

Lebel, L. L.; Aissa, B.; Paez, O. A.; El Khakani, M. A. & Therriault, D. (2009). Three-dimensional micro structured nanocomposite beams by microfluidic infiltration. *Journal of Micromechanics and Microengineering*, Vol. 19, No. 12, (December 2009) 125009 (7 pp.), 0960-1317

Lewis, J. A. & Gratson, G. M. (2004). Direct writing in three dimensions. *Materials Today*, Vol. 7, No. 7, (July/August 2004) 32-39, 1369-7021

Li, D. & Xia, Y. (2004). Electrospinning of Nanofibers: Reinventing the Wheel? *Advanced Materials*, Vol. 16, No. 14, (July 2004) 1151-1170, 1521-4095

Mamedov, A. A.; Kotov, N. A.; Prato, M.; Guldi, D. M.; Wicksted, J. P. & Hirsch, A. (2002). Molecular design of strong single-wall carbon nanotube/polyelectrolyte multilayer composites. *Nature Materials*, Vol. 1, No. 3, (November 2002) 190-194, 1476-1122

Miaudet, P.; Bartholome, C.; DerrÈ, A.; Maugey, M.; Sigaud, G.; Zakri, C. & Poulin, P. (2007). Thermo-electrical properties of PVA-nanotube composite fibers. *Polymer*, Vol. 48, No. 14, (June 2007) 4068-4074, 0032-3861

Minus, M. L.; Chae, H. G. & Kumar, S. (2009). Interfacial crystallization in gel-spun poly (vinyl alcohol)/single-wall carbon nanotube composite fibers. *Macromolecular Chemistry and Physics*, Vol. 210, No. 21, (November 2009) 1799-1808, 1022-1352

O'Connell, M. J.; Boul, P.; Ericson, L. M.; Huffman, C.; Wang, Y.; Haroz, E.; Kuper, C.; Tour, J.; Ausman, K. D. & Smalley, R. E. (2001). Reversible water-solubilization of single-walled carbon nanotubes by polymer wrapping. *Chemical Physics Letters*, Vol. 342, No. 3-4, (July 2001) 265-271, 0009-2614

Raghavan, S. R.; Walls, H. J. & Khan, S. A. (2000). Rheology of silica dispersions in organic liquids: New evidence for solvation forces dictated by hydrogen bonding. *Langmuir*, Vol. 16, No. 21, (October 2000) 7920-7930, 0743-7463

Sahoo, N. G.; Jung, Y. C.; Yoo, H. J. & Cho, J. W. (2006). Effect of functionalized carbon nanotubes on molecular interaction and properties of polyurethane composites. *Macromolecular Chemistry and Physics*, Vol. 207, No. 19, (October 2006) 1773-1780, 1022-1352

Sainz, R.; Benito, A. M.; Martinez, M. T.; Galindo, J. F.; Sotres, J.; Baro, A. M.; Corraze, B.; Chauvet, O. & Maser, W. K. (2005). Soluble self-aligned carbon nanotube/polyaniline composites. *Advanced Materials*, Vol. 17, No. 3, (Fabruary 2005) 278-281, 0935-9648

Sandler, J. K. W.; Pegel, S.; Cadek, M.; Gojny, F.; Van Es, M.; Lohmar, J.; Blau, W. J.; Schulte, K.; Windle, A. H. & Shaffer, M. S. P. (2004). A comparative study of melt spun polyamide-12 fibres reinforced with carbon nanotubes and nanofibres. *Polymer*, Vol. 45, No. 6, (March 2004) 2001-2015, 0032-3861

Satake, A.; Miyajima, Y. & Kobuke, Y. (2005). Porphyrin-carbon nanotube composites formed by noncovalent polymer wrapping. *Chemistry of Materials*, Vol. 17, No. 4, (February 2005) 716-724, 0897-4756

Starr, F. W.; Schrder, T. B. & Glotzer, S. C. (2002). Molecular dynamics simulation of a polymer melt with a nanoscopic particle. *Macromolecules*, Vol. 35, No. 11, (May 2002) 4481-4492, 0024-9297

Stoeffler, K.; Perrin-Sarazin, F.; That, M. T. T. & Denault, J. (2010). Polyethylene/Carbon Nanotubes Nanocomposites, *Proceedings of 8th Joint Canada-Japan Workshop on Composites*, Montreal, Canada, July 26-29, 2010, DEStech Publications Inc, In Press

Therriault, D.; Shepherd, R. F.; White, S. R. & Lewis, J. A. (2005). Fugitive inks for direct-write assembly of three-dimensional microvascular networks. *Advanced Materials*, Vol. 17, No. 4, (February 2005) 395-399, 0935-9648

Therriault, D.; White, S. R. & Lewis, J. A. (2003). Chaotic mixing in three-dimensional microvascular networks fabricated by direct-write assembly. *Nature Materials*, Vol. 2, No. 4, (April 2003) 265-271, 1476-1122

Thostenson, E. T. & Chou, T.-W. (2002). Aligned multi-walled carbon nanotube-reinforced composites: Processing and mechanical characterization. *Journal of Physics D: Applied Physics*, Vol. 35, No. 16, (August 2002) 77-80, 0022-3727

Thostenson, E. T. & Chou, T.-W. (2006). Carbon nanotube networks: Sensing of distributed strain and damage for life prediction and self healing. *Advanced Materials*, Vol. 18, No. 21, (November 2006) 2837-2841, 0935-9648

Tsurumi, T. (1994). Solution Spinning. In: *Advanced fiber spinning technology*. Nakajima, T., Kajiwara, K. & McIntyre , J. E. (Ed.). 1-24. Woodhead Publishing Ltd., 1-85573-182-7, Cambridge, England

Varadan, V. K. & Varadan, V. V. (2001). Micro stereo lithography for fabrication of 3D polymeric and ceramic MEMS, *Proceedings of The International Society for Optical Engineering - MEMS Design, Fabrication, Characterization, and Packaging*, 978-0-8194-4108-9, Edinburgh, United kingdom, May/June 2001, SPIE,

Varadan, V. K.; Xie, J. & Ji, T. (2001). Three dimensional MEMS devices with functionalized carbon nanotubes, *Proceedings of The International Society for Optical Engineering, Micromachining and Microfabrication Process Technology VIII*, 978-0-8194-4779-1, Adelaide, Australia, January 2003, SPIE,

Winey, K. I. & Vaia, R. A. (2007). Polymer nanocomposites. *MRS Bulletin*, Vol. 32, No. 4, (April 2007) 314-319, 0883-7694

Wong, M.; Paramsothy, M.; Xu, X. J.; Ren, Y.; Li, S. & Liao, K. (2003). Physical interactions at carbon nanotube-polymer interface. *Polymer*, Vol. 44, No. 25, (December 2003) 7757-7764, 0032-3861

Xu, M.; Zhang, T.; Gu, H.; Wu, J. & Chen, Q. (2006). Synthesis and properties of novel polyurethane - Urea/multiwalled carbon nanotube composites. *Macromolecules*, Vol. 39, No. 10, (May 2006) 3540-3545, 0024-9297

Xu, X.; Thwe, M. M.; Shearwood, C. & Liao, K. (2002). Mechanical properties and interfacial characteristics of carbon-nanotube-reinforced epoxy thin films. *Applied Physics Letters*, Vol. 81, No. 15, (October 2002) 2833-5, 0003-6951

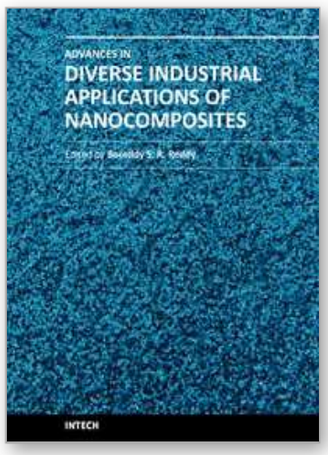

Advances in Diverse Industrial Applications of Nanocomposites

Edited by Dr. Boreddy Reddy

ISBN 978-953-307-202-9
Hard cover, 550 pages
Publisher InTech
Published online 22, March, 2011
Published in print edition March, 2011

Nanocomposites are attractive to researchers both from practical and theoretical point of view because of combination of special properties. Many efforts have been made in the last two decades using novel nanotechnology and nanoscience knowledge in order to get nanomaterials with determined functionality. This book focuses on polymer nanocomposites and their possible divergent applications. There has been enormous interest in the commercialization of nanocomposites for a variety of applications, and a number of these applications can already be found in industry. This book comprehensively deals with the divergent applications of nanocomposites comprising of 22 chapters.

How to reference

In order to correctly reference this scholarly work, feel free to copy and paste the following:

Louis Laberge Lebel and Daniel Therriault (2011). Multiscale Manufacturing of Three-Dimensional Polymer-Based Nanocomposite Structures, Advances in Diverse Industrial Applications of Nanocomposites, Dr. Boreddy Reddy (Ed.), ISBN: 978-953-307-202-9, InTech, Available from: http://www.intechopen.com/books/advances-in-diverse-industrial-applications-of-nanocomposites/multiscale-manufacturing-of-three-dimensional-polymer-based-nanocomposite-structures

INTECH
open science | open minds

InTech Europe
University Campus STeP Ri
Slavka Krautzeka 83/A
51000 Rijeka, Croatia
Phone: +385 (51) 770 447
Fax: +385 (51) 686 166
www.intechopen.com

InTech China
Unit 405, Office Block, Hotel Equatorial Shanghai
No.65, Yan An Road (West), Shanghai, 200040, China
中国上海市延安西路65号上海国际贵都大饭店办公楼405单元
Phone: +86-21-62489820
Fax: +86-21-62489821

IntechOpen